

Computational physics approaches to light transmission through a twisted nematic liquid crystal slab

Nadina Gheorghiu and George Y. Panasyuk

January 24, 2018

Abstract

We consider light propagation through a twisted nematic liquid crystal. At first, an expression for light transmission is obtained using a rather intuitive approach. Secondly, an accurate solution for light transmission based on Maxwell's equations is derived and compared with the previous one. Both approaches show that when changes in the orientation of the liquid crystal optical axis are small on the scale defined by the optical wavelength (Mauguin limit), the polarization of light approximately follows the optical axis. At the same time, even in this limit, the simple formula for the light transmittance mentioned in some monographs on liquid crystal displays is not necessary accurate. Conditions under which the two approaches give the same expression for the light transmission are found. In addition, two numerical methods for finding the light transmittance are considered. It is demonstrated that the Gauss-Seidel method has much faster convergence rate than the Euler method.

1 Introduction

As their name suggests, liquid crystals (LCs), in particular nematic liquid crystals (NLCs) that we consider here, are mesophases between the liquid and the crystalline states of matter [1]. LCs can flow like ordinary fluids, yet they also display an orientational long-range order, which is due to the anisotropic, rod-like shape of molecules. This *intrinsic anisotropy* of NLCs can be described by a unit vector $\mathbf{n}(\mathbf{r})$, called the *director*, aligned along the direction of preferred orientation of the molecules at a space point \mathbf{r} (Fig. 1). The states \mathbf{n} and $-\mathbf{n}$ are indistinguishable, since the same number of molecules orient, on average, along each of these directions. There are three elastic deformations that can occur in the bulk of an uniaxial nematic (Fig. 2). The director alignment can be imposed along a particular direction by special treatment of the glass electrodes confining the LC. Assuming no abrupt changes or singularities (points or lines), the director deformations can be described within the continuum theory [1]. Thus, LCs are not ordinary fluids. Optical patterns of NLCs subjected to electric and magnetic fields show the very complex nature and behavior of these systems [2]. The delicate balance between rigidity and fluidity makes LCs perfect components of biological systems [3, 4]. It was found that short DNA

oligomers can form LC phases by a mechanism responsible for prebiotic formation of DNA molecules on primordial Earth [5]. At higher DNA concentration, the higher-order columnar LC phase¹ was found to exhibit dendritic growth forms, indicative of lower symmetry and a more solid-like ordering. Mostly known for their use in the display industry, LCs are unique in the diversity of their properties [6]. For instance, the existence of LC order in iron-based superconductors was experimentally proved by neutron scattering studies that showed the role played by the magnetic degrees of freedom in driving the formation of electronic LCs [7]. Quantum fluctuations in solid state lattices give rise to electronic LC states, which break the rotational symmetry of the lattice while partially preserving its translational symmetry [8].

Maxwell's equations are central to the description of light propagation through LCs. Likewise the case of all other equations from mathematical physics, solutions to Maxwell's equation for two- or three-dimensional problems have become available only with the advent of fast computers and, especially, computational algorithms. Many problems are still not amenable to even the modern computer power. Therefore, the development of both analytical and computational methods as well as the ability to optimally combine them is essential for the task of finding both accurate and less time-consuming solutions to physics problems. As Maxwell himself once wrote: "... the aim of exact science is to reduce the problems of nature to the determination of quantities by operations with numbers."

To illustrate these general ideas, we choose here an example from LC optics. There are two problems that often arise in any LC study. The first problem is to find the director field $\mathbf{n}(\mathbf{r})$ everywhere within the LC cell volume, which can be done by minimizing the corresponding (Frank-Oseen) free energy [1]. The second problem is to calculate light transmittance through the LC cell by solving Maxwell's equations. Generally, these can be complicated problems and time-effective methods are needed in order to tackle them. Despite the fact that in the vast majority of cases only numerical solutions are available, we show here an interesting and, at the same time, non-trivial example of analytical solution to the problem of calculating the light transmittance through a LC slab with known (helical) director structure.

2 Light transmission through a twisted nematic liquid crystal layer

Consider the propagation of an electromagnetic wave of optical frequency ω that enters along the perpendicular direction a LC slab of thickness d . The bounding plates (Fig. 3) impose the boundary conditions for the director alignment: $\mathbf{n}(0) = \mathbf{x}$ and $\mathbf{n}(d) = \mathbf{y}$. Intuitively, one can suggest that in order to minimize its energy the NLC will acquire a helical structure along the normal direction \mathbf{z} to the layer:

$$\mathbf{n}(z) = \cos(qz)\mathbf{x} + \sin(qz)\mathbf{y}, \quad (1)$$

where $q = \pi/2d$, \mathbf{x} , \mathbf{y} , and \mathbf{z} are the unit vectors along the axes of the laboratory coordinate system xyz , while $z = 0$ is where the electromagnetic wave enters the LC layer. As one can easily verify, a simple mathematical approach of the problem brings exactly the same result [1]. Addition of two polarizers (A

and P, shown in Fig. 3) to the LC slab results in what is widely known as an essential part of a twisted nematic liquid crystal (TNLC) display. We assume for simplicity that no electric or magnetic field are applied on the TNLC, apart from the time-varying electric and magnetic fields in the (electromagnetic) optical wave interacting with the TNLC. Since the director \mathbf{n} cannot follow the high frequency oscillations in the incoming electromagnetic wave, its helical structure remains stationary.

The next step is to find the amount of light transmitted through the TNLC layer. After passing through the entrance linear polarizer (P), only the x component of the electric field in the electromagnetic wave will survive. While advancing through the TNLC layer, the electric field of the wave will acquire also a y component. The reason for this is that the optical axis (director) \mathbf{n} rotates in accordance to Eq. 1. To describe quantitatively this wave propagation, we assume that changes in \mathbf{n} on the scale of the optical wavelength λ are small. The imposed condition $\lambda \ll d$ is satisfied only approximately, as usually $d \geq 5\mu\text{m}$. In this case, we can divide the TNLC layer into $N \gg 1$ thin sheets. Inside each of these sheets, \mathbf{n} is a constant vector rotated by a small angle $\delta\phi$ with respect to the preceding sheet. The electric component \mathbf{E}_m of the electromagnetic field after exiting the m -th sheet can be generally written, in general, as a vector sum

$$\mathbf{E}_m = E_{m\parallel}\mathbf{n}_m + E_{m\perp}\mathbf{s}_m \quad (2)$$

where the unit vector \mathbf{s}_m lies in the xy -plane, $\mathbf{s}_m \perp \mathbf{n}_m$, and \mathbf{n}_m is the director in the m -th sheet. In this way, $\mathbf{E}_{m\perp}$ is called the *ordinary* component and $\mathbf{E}_{m\parallel}$ is called the *extraordinary* component. The two waves propagate with speeds $v_o = c/n_o$ and $v_e = c/n_e$, respectively, where n_o and n_e are the ordinary and the extraordinary indexes of refraction and c is the speed of light in vacuum. On the other hand, \mathbf{E}_m can be also written as

$$\mathbf{E}_m = E'_{m\parallel}\mathbf{n}_{m+1} + E'_{m\perp}\mathbf{s}_{m+1} \quad (3)$$

Equating the two expressions for \mathbf{E}_m (Eqs. 2,3) and projecting both sides on the \mathbf{n}_{m+1} and \mathbf{s}_{m+1} directions, we come up with the following expressions for the ordinary and extraordinary components at the exit of the $(m+1)$ -th sheet

$$\begin{aligned} E_{m+1,\perp} \equiv E'_{m\perp} &= E_{m\parallel} \sin(\delta\phi) + E_{m\perp} \cos(\delta\phi) \\ E_{m+1,\parallel} \equiv E'_{m\parallel} e^{id\Phi} &= [E_{m\parallel} \cos(\delta\phi) - E_{m\perp} \sin(\delta\phi)] e^{id\Phi} \end{aligned} \quad (4)$$

The phase factor $e^{id\Phi}$ appears due to the difference between v_o and v_e . Here $d\Phi = k_0(\Delta n)dz$, where $k_0 = 2\pi/d$ and $\Delta n = n_e - n_o$ is called the NLC's *birefringence*. Assuming that $dz = d/N$ is infinitesimally small (when $N \rightarrow \infty$), one obtains the following system of equations for the ordinary and extraordinary components

$$\begin{aligned} \frac{dE_{\perp}(z)}{dz} &\equiv E'_{\perp}(z) = k_0 E_{\parallel}(z) \\ \frac{dE_{\parallel}(z)}{dz} &\equiv E'_{\parallel}(z) = ik_0(\Delta n)E_{\parallel}(z) - k_0 E_{\perp}(z) \end{aligned} \quad (5)$$

The light transmission coefficient is determined as the ratio of the transmitted, I_T , to the incident, I_I , intensity⁷

$$T = \frac{I_T}{I_I} = \left(\frac{|E_{0T}|}{|E_{0I}|} \right)^2, \quad (6)$$

where E_{0I} and E_{0T} are the amplitudes of the electric field at the incidence and at the exit from the TNLC slab, respectively. Analytical solution of this system of partial ordinary differential equations (ODEs) with boundary conditions $E_{\perp}(0) = 0$ and $E_{\parallel}(0) = 1$ (to avoid normalization by $|E_{0I}|^2$) can be easily found. Keeping only the relevant component, we arrive at:

$$E_{\perp}(z) = e^{i\pi gz/2d} \sin\left(\frac{\pi\sqrt{g^2+1}z}{2d}\right) \left(\sqrt{g^2+1}\right)^{-1} \quad (7)$$

Taking into account the presence of the analyzer (A), the light transmission coefficient will be determined by⁸:

$$T(g) = |E_{\perp}(d)|^2 = \frac{\sin^2[\pi(g^2+1)^{1/2}/2]}{g^2+1} \quad (8)$$

where $g = 2d(\Delta n)/\lambda$ is a dimensionless parameter. For large values of g , which is consistent with our initial supposition that $d \gg \lambda$, light transmittance given by Eq. 8 approaches zero. It can be explained by assuming that the electric field component in the polarized light is aligned approximately along the director. In this situation, its x -component is small, i.e. $|E_x(d)|^2 = |E_{\perp}(d)|^2 \simeq 0$. This assumption will be fully proved in the next section. As will be shown, the polarization of light propagating through the LC slab indeed follows the director in the Mauguin limit [11] provided that $g \gg 1$ (see Eq. 29). When $g = 0$, the result ($T(g = 0) = 1$) is also correct: if, for example, $d = 0$ or $\Delta n = 0$, there is no slab at all or the slab does not change the polarization of the incoming light. However, for intermediate values of g ($g \leq 1$), Eq. 8 might not be correct, and a more accurate solution presented in the next section should be invoked.

3 Analytical solution to light propagation based on Maxwell's equations

We start from the wave equation

$$\nabla(\nabla\mathbf{E}) - \nabla^2\mathbf{E} = -\frac{1}{c^2} \frac{\partial^2\mathbf{D}}{\partial t^2} \quad (9)$$

which can be obtained by eliminating the magnetic component of the electromagnetic field from Maxwell's equations [9, 12]. Here \mathbf{D} is the displacement vector and, as before, \mathbf{E} is the electric field component of the wave. The intrinsic anisotropy of LCs makes the relation between \mathbf{D} and \mathbf{E} dependent on the orientation of \mathbf{E} with respect to \mathbf{n} , namely $\mathbf{D} = \epsilon_{\perp}\mathbf{E}$ for $\mathbf{E} \perp \mathbf{n}$ and $\mathbf{D} = \epsilon_{\parallel}\mathbf{E}$ for $\mathbf{E} \parallel \mathbf{n}$. In the general case, \mathbf{E} is not necessarily parallel to \mathbf{D} and the relation between \mathbf{D} and \mathbf{E} is^{1,4}

$$\mathbf{D} = \epsilon_{\perp}\mathbf{E} + \Delta\epsilon \cdot \mathbf{n}(\mathbf{n}\mathbf{E}) \quad (10)$$

where $\Delta\epsilon = \epsilon_{\parallel} - \epsilon_{\perp}$ is the anisotropy in the dielectric constant. The homogeneity in the xy plane requires $\partial_{x,y}\mathbf{E} = \mathbf{0}$. Also, because $\mathbf{n}\perp\mathbf{z}$, $D_z = 0$. Thus, looking for a solution of Eq. 9 in the form $\mathbf{E}(z, t) = \mathbf{E}(z)e^{-i\omega t}$, where $\mathbf{E}(z) = [E_x(z), E_y(z)]$, Eq. 9 reduces to:

$$\begin{aligned} -E_x''(z) &= k_0^2 [\epsilon_{\perp} E_x + \Delta\epsilon \cdot n_x (n_x E_x + n_y E_y)] \\ -E_y''(z) &= k_0^2 [\epsilon_{\perp} E_y + \Delta\epsilon \cdot n_y (n_x E_x + n_y E_y)] \end{aligned} \quad (11)$$

Taking into account Eq. 1, Eqs. (11) can be written as:

$$\begin{aligned} -E_x'' &= k_0^2 \bar{\epsilon} E_x + \frac{1}{2} k_0^2 \Delta\epsilon [\cos(2qz) E_x + \sin(2qz) E_y] \\ -E_y'' &= k_0^2 \bar{\epsilon} E_y + \frac{1}{2} k_0^2 \Delta\epsilon [\sin(2qz) E_x - \cos(2qz) E_y] \end{aligned}$$

where $\bar{\epsilon} = (\epsilon_{\parallel} + \epsilon_{\perp})/2$. Using the Euler representation for trigonometric functions, the previous system of equations can be rewritten in terms of the new variables $E_{1,2}(z) = E_x(z) \pm iE_y(z)$ as

$$\begin{aligned} -E_1'' &= \frac{1}{2} k_0^2 (\Delta\epsilon) e^{2iqz} E_2 + k_0^2 \bar{\epsilon} E_1 \\ -E_2'' &= k_0^2 \bar{\epsilon} E_2 + \frac{1}{2} k_0^2 (\Delta\epsilon) e^{-2iqz} E_1 \end{aligned} \quad (12)$$

Note that Eqs. 12 accurately describe propagation of an electromagnetic wave normally incident to the TNLC layer. Looking for a solution of Eqs. 12 in the form

$$E_{1,2}(z) = E_{01,02} e^{i(k\pm q)z}, \quad (13)$$

we arrive at the following linear equations with respect to $E_{01,02}$:

$$[(k+q)^2 - k_0^2 \bar{\epsilon}] E_{01} = \frac{1}{2} k_0^2 \Delta\epsilon E_{02}, \quad (14)$$

$$\frac{1}{2} k_0^2 \Delta\epsilon E_{01} = [(k-q)^2 - k_0^2 \bar{\epsilon}] E_{02}, \quad (15)$$

and a non-trivial solution for $E_{01,02}$ is only possible if the determinant vanishes, which gives the following *dispersion relation*:

$$(k^2 + q^2 - k_0^2 \bar{\epsilon})^2 = 4q^2 k^2 + k_0^4 \left(\frac{\Delta\epsilon}{2} \right)^2 \quad (16)$$

between ω (or $k_0 = \omega/c$) and the wave number $k = k(\omega)$ of the propagating wave.

Eq. 16 has four solutions. Two of these solutions, which we denote by $k^{(o,+)} = k^{(o,+)}(\omega)$ and $k^{(e,+)} = k^{(e,+)}(\omega)$, correspond to the two waves propagating in the positive direction of the z -axis. The other two, with $k^{(o,-)} = -k^{(o,+)}$ and $k^{(e,-)} = -k^{(e,+)}$, correspond to the two waves traveling in the opposite direction. For convenience, we introduce the index m standing for “o” or “e” and the index s corresponding to either “+” or “-” (forward- or back-propagating wave). For each $k^{(m,s)}$, we can find the ratio $r^{(m,s)} = E_{02}^{(m,s)}/E_{01}^{(m,s)}$ of the corresponding amplitudes using, for example, Eq. 14. Eq. 14 and Eq. 15 become equivalent if $k(\omega)$ satisfies Eq. 16.

A general solution for the electric component \mathbf{E} of the electromagnetic field in the LC layer will be a superposition of these four modes and can be presented as:

$$\mathbf{E} = \sum_{m,s} \left[\mathbf{x}E_x^{(m,s)}(z) + \mathbf{y}E_y^{(m,s)}(z) \right] = \sum_{m,s} \left[\mathbf{e}_1 E_{01}^{(m,s)} e^{iqz} + \mathbf{e}_2 E_{02}^{(m,s)} e^{-iqz} \right] e^{ik^{(m,s)}z}, \quad (17)$$

where $\mathbf{e}_{1,2} = (\mathbf{x} \mp i\mathbf{y})/2$. Thus, there are four contributions in each sum. As is known, each of these solutions represent an elliptically polarized wave [12]. The axes of the ellipse, x' and y' , are rotated by an angle $\phi = qz$ with respect the lab coordinates x and y . As one can notice immediately from Fig. 1, this angle coincides with the director angle. Finally, the ratio μ of the rotated ellipse semiaxes (along x' and y') is $\mu^{(m,s)} = |(1 + r^{(m,s)})/(1 - r^{(m,s)})|$.

Let us restrict our attention to the visible wavelengths, when $\lambda = 2\pi/k \sim 0.5 \mu\text{m}$. This wavelength region is the most important for the LC physics, in particular for LC displays. Taking into account that typical values for the helical pitch $p = 2\pi/q = 4d \sim 10 \div 100 \mu\text{m}$, the ratio q/k is small. It allows for an expansion of all relations in terms of this ratio and keeping only its first order. With this approximation, Eq. 16 gives the following solutions:

$$\begin{aligned} k^{(o,\pm)} &= \pm k_0 n_o + O(\delta^2) \\ k^{(e,\pm)} &= \pm k_0 n_e + O(\delta^2), \end{aligned} \quad (18)$$

where $k_0 = \omega/c$. As follows from Eq. 14, the corresponding ratios $r^{(m,s)}$ are determined as:

$$r^{(o,\pm)} = -1 \pm a_o \delta + O(\delta^2), \quad r^{(e,\pm)} = 1 \pm a_e \delta + O(\delta^2) \quad (19)$$

$$a_o = \frac{2n_o}{n_o + n_e}, \quad a_e = \frac{2n_e}{n_o + n_e}, \quad \delta = \frac{\lambda}{2d\Delta n} = g^{-1} \quad (20)$$

As is clear, $\mu^{(o,\pm)} = |(1 + r^{(o,\pm)})/(1 - r^{(o,\pm)})| \approx a_o \delta / 2$. For small δ , these parameters describe the ordinary waves propagating in the forward or backward direction, respectively. Both of them are polarized approximately along the y' -axis, which is perpendicular to the director at any point inside the slab. In the second case, $\mu^{(e,\pm)} \approx 2/(a_e \delta)$ and we have the extraordinary waves approximately polarized along the x' -axis, which is parallel to the director. The electric component $\mathbf{E}_t = (E_{tx}, E_{ty})$ of the forward-propagating (transmitted) wave is a superposition of the ordinary and extraordinary waves, traveling in the positive direction of the z -axis. Taking $s = "+"$ in Eq. 17, the forward-propagating wave can be presented as:

$$E_{tx} = \frac{1}{2} \sum_m \left\{ E_{02}^{(m,+)} e^{i[k^{(m,+)} - q]z} + E_{01}^{(m,+)} e^{i[k^{(m,+)} + q]z} \right\} \quad (21)$$

$$E_{ty} = \frac{i}{2} \sum_m \left\{ E_{02}^{(m,+)} e^{i[k^{(m,+)} - q]z} - E_{01}^{(m,+)} e^{i[k^{(m,+)} + q]z} \right\}. \quad (22)$$

In the same way, the electric component $\mathbf{E}_r = (E_{rx}, E_{ry})$ of the back-propagating (reflected) wave is a superposition of the ordinary and extraordinary waves, traveling in the negative direction of the z -axis. The back-propagating wave can be

presented as:

$$E_{rx} = \frac{1}{2} \sum_m \left\{ E_{02}^{(m,-)} e^{i[k^{(m,-)}-q]z} + E_{01}^{(m,-)} e^{i[k^{(m,-)}+q]z} \right\} \quad (23)$$

$$E_{ry} = \frac{i}{2} \sum_m \left\{ E_{02}^{(m,-)} e^{i[k^{(m,-)}-q]z} - E_{01}^{(m,-)} e^{i[k^{(m,-)}+q]z} \right\}. \quad (24)$$

Using the definition of the ratio $r^{(m,s)}$, we can express \mathbf{E}_t and \mathbf{E}_r through only four unknowns $E_{01}^{(m,s)}$:

$$\begin{aligned} E_{tx} &= \frac{1}{2} \sum_m E_{01}^{(m,+)} \left\{ r^{(m,+)} e^{i[k^{(m,+)}-q]z} + e^{i[k^{(m,+)}+q]z} \right\} \\ E_{ty} &= \frac{i}{2} \sum_m E_{01}^{(m,+)} \left\{ r^{(m,+)} e^{i[k^{(m,+)}-q]z} - e^{i[k^{(m,+)}+q]z} \right\} \end{aligned} \quad (25)$$

$$\begin{aligned} E_{rx} &= \frac{1}{2} \sum_m E_{01}^{(m,-)} \left\{ r^{(m,-)} e^{i[k^{(m,-)}-q]z} + e^{i[k^{(m,-)}+q]z} \right\} \\ E_{ry} &= \frac{i}{2} \sum_m E_{01}^{(m,-)} \left\{ r^{(m,-)} e^{i[k^{(m,-)}-q]z} - e^{i[k^{(m,-)}+q]z} \right\} \end{aligned} \quad (26)$$

where $r^{(m,s)}$ are determined by Eqs. 19, 20 in the considered approximation.

The corresponding magnetic components, \mathbf{H}_t and \mathbf{H}_r , can be easily found from Eqs. 25, 26 and relations

$$\mathbf{H}_{t,r} = \frac{i}{k_0} (\mathbf{x} \partial_z E_{t,ry} - \mathbf{y} \partial_z E_{t,rx}). \quad (27)$$

To properly take into account both the polarizer (P)- and analyzer (A)-LC interfaces, one has to introduce a plane wave ($\mathbf{E}_r^{(P)}$, $\mathbf{H}_r^{(P)}$) reflected from the P-LC interface and a plane wave ($\mathbf{E}_t^{(A)}$, $\mathbf{H}_t^{(A)}$) transmitted through the LC-A interface. It will bring four additional unknown constants, analogous to $E_{01}^{(n,s)}$, and all eight constants can be determined from continuity of the tangential (x and y) components of the electric and magnetic fields at both interfaces. As a result, the light transmittance will depend on the refraction indexes of both polarizer n_P and analyzer n_A . At the same time, reflected light was not considered in the simple derivation of light transmittance discussed in the previous section. It means that Eq. 8, strictly speaking, is not correct even in the limit of small δ . Let us, nevertheless, find conditions under which Eq. 8 is still valid.

In many practical situations, $\Delta n \propto 0.1$ and reflections are small if one chooses $n_o \leq \text{Re}(n_{P,A}) \leq n_e$. Indeed, the reflection coefficient \bar{r} , defined by the relation $\mathbf{E}_r = \bar{r} \mathbf{E}_{inc}$ [12], will be of the order of $\bar{r} \propto \Delta n / 2n_e$ and therefore small. As is also clear, back-propagating wave, which is a wave reflected from the LC layer itself, will be also of the order of \bar{r} , or even of a higher order. Indeed, the back-scattered wave appears because the optical axis (director) varies with the z -coordinate. In this case we can divide the whole LC slab into a number of thin sheets (as it was done in the previous section) and consider also reflections at each of these interfaces. If the birefringence goes to zero, the slab

will become homogeneous in the z -direction, these reflections will disappear, and \mathbf{E}_r in Eq. 26 will vanish. Thus, to simplify our consideration and make possible the comparison to the results from previous section, we consider the following situation. Assume that the real part of the either polarizer's and analyzer's index of refraction is equal to the extraordinary index of refraction, i.e. $\text{Re}(n_{P,A}) = n_e$. The imaginary part of $n_{A,P}$ is of the order of $10^{-5} - 10^{-3}$ and therefore negligible. In this case, one can neglect the reflection of the incident wave from the P-LC interface that is polarized along the director at the beginning of the LC layer (at $z = 0$). We may also suppose, based on our previous simple consideration, that the wave propagating through the LC approximately follows the helix. It means that its largest component, which is polarized along the y -axis at the end of the LC layer, will pass the LC-A interface essentially without reflection. The other (small) component that is polarized along the x -axis, will be reflected. Thus, we have waves that are reflected from both LC layer and LC-A interface that are proportional to the small factor \bar{r} . These waves will hit the LC-P interface and again will be reflected back to the LC layer. As is clear, these waves will contribute to the transmitted radiation, but their amplitudes will be proportional to the small factor \bar{r}^2 . If we are not interested in these small corrections, we may consider only the forward-propagating wave (Eq. 25), disregarding the back-propagating wave (Eq. 26) and also reflections from the LC-A interface. These simplifying assumptions allow us to compare the result that we will obtain in this section with the light transmittance derived in the previous section.

Using Eq. 25, one can obtain the unknown values $E_{01}^{(n,+)}$ from the following equations: $E_{tx}(z = 0) = 1$ and $E_{ty}(z = 0) = 0$. Neglecting $O(\delta^2)$ contributions, one can easily find:

$$E_{01}^{(o,+)} = \frac{1}{2}a_e\delta, \quad E_{01}^{(e,+)} = 1 - \frac{1}{2}a_e\delta. \quad (28)$$

Substitution of these expressions into Eq. 25 gives:

$$\mathbf{E}_t(z) = \mathbf{n}(z)e^{ik_0n_eyz} + \frac{i}{2}a_e\delta(e^{ik_0n_oz} - e^{ik_0n_eyz})[\mathbf{x}\sin(qz) - \mathbf{y}\cos(qz)]. \quad (29)$$

Corresponding expressions for the magnetic components of the transmitted wave can be obtained from Eq. 27. In particular,

$$H_{ty}(z) = n_e \cos(qz) e^{ik_0n_eyz} + \frac{i}{2}a_e\delta[n_oe^{ik_0n_oz} - e^{ik_0n_eyz}(n_e a_e - \Delta n)]\sin(qz). \quad (30)$$

As is known¹¹, the light transmittance T through the LC layer can be calculated as

$$T = \frac{|\mathbf{S}_d \cdot \mathbf{z}|}{|\mathbf{S}_0 \cdot \mathbf{z}|}, \quad (31)$$

where $\mathbf{S}_{0,d}$ are the values of the Poynting vector at the beginning ($z = 0$) and at the end ($z = d$) of the LC slab. In this case, because of the choice of directions for light transmitted through the analyzer and polarizer, we have:

$$\mathbf{z} \cdot \mathbf{S}_{0,d} = \frac{c}{8\pi} E_{tx} H_{ty}^*|_{z=0,d}. \quad (32)$$

Using Eq. 30, one finds that $E_{tx}(0)H_{ty}^*(0) = n_e$. Taking into account that $qd = \pi/2$, $e^{\pm i\pi/2} = \pm i$, $k_0\Delta nd = \pi/\delta$, Eq. 31 can be transformed to

$$T \equiv T_{\perp} = \frac{1}{4n_e} a_e \delta^2 (1 - e^{i\pi/\delta}) [a_e n_e - (a_e n_e - \Delta n) e^{-i\pi/\delta}]. \quad (33)$$

Using Eq. 20 for a_e and observing that

$$n_e a_e - \Delta n = \frac{2n_e n_o}{n_e + n_o} + O(\Delta n)^2, \quad (34)$$

one can rewrite Eq. 33 as

$$T_{\perp} = \frac{a_e^2 \delta^2 n_o}{n_e} \sin^2 \frac{\pi}{2\delta}. \quad (35)$$

Within our approximation, small corrections of the order of $O(\Delta n)^2 \propto \bar{r}^2$ have been neglected. In the same way,

$$(n_e + n_o)^2 = 4n_e n_o + O(\Delta n)^2 \quad (36)$$

and one can represent Eq. 35 in the form:

$$T_{\perp} = \delta^2 \sin^2 \frac{\pi}{2\delta} \quad (37)$$

which coincides with the result (Eq. 8) found in the previous section for the case of large $g = \delta^{-1}$ (Mauguin limit). As is also clear from Eq. 29, in the limit of small $\delta = 1/g$ the polarization of light indeed approximately follows the director (optical axis) \mathbf{n} .

4 Computational

As we have already discussed, Eq. 8 for the light transmittance is not accurate. Using the analytical approach based on Maxwell's equations, one can obtain an expression for the light transmittance valid for all g . However, for vast majority of situations, when the director does not obey simple formulas like (1) or for the case of oblique incidence of an electromagnetic wave, it is not possible to derive an accurate analytical expression for the light transmittance. For example, in the considered TN mode and for a nonzero electric field, the light transmittance can be obtained only by numerical solving of the corresponding equations. This is even more true for cases when the director $\mathbf{n} = \mathbf{n}(\mathbf{r})$ has a three-dimensional structure. varies along all space directions. Despite the lack of analytical formulas, there is usually an excellent correspondence between numerical solutions to these problems and measurements of the light transmittance provided that the numerical solver is accurate and fast enough. This often enables one, for example, to optimize the performance of a LC display avoiding thousands or sometimes even millions of costly measurements.

In this Section we show two numerical approaches, Euler and Gauss-Seidel, for solving ODEs like Eqs. 5 and demonstrate the advantage of the latter one. Consider a system of N first-order linear ODEs to determine an N -component

vector $\mathbf{E}(z)$ on an interval $a \leq z \leq b$ with known $\mathbf{E}(a)$. This system can always be written in the matrix form

$$\mathbf{E}'(z) = \frac{d}{dz}\mathbf{E} = A \cdot \mathbf{E}, \quad (38)$$

where $A \equiv A(z)$ is a known matrix. For our system (5), all matrix coefficients are z independent: $A_{11} = 0$, $A_{12} = k_0$, $A_{21} = -k_0$, and $A_{22} = ik_0\Delta h$. The Euler method for numerically solving Eq. 38 consists of a step-by-step application of the formula

$$\mathbf{E}(z + dz) = \mathbf{E}(z) + A(z) \cdot \mathbf{E}(z)dz = [I + A(z)dz] \mathbf{E}(z), \quad (39)$$

where I is the $N \times N$ unit matrix and $dz = d/N$ is the mesh step. Alternatively, the Gauss-Seidel (GS) method consists of solving the equation

$$\mathbf{E}(z + dz) = \mathbf{E}(z) + \frac{1}{2} [A(z + dz) \cdot \mathbf{E}(z + dz) + A \cdot \mathbf{E}(z)] dz \quad (40)$$

with respect to $\mathbf{E}(z + dz)$ for each step. Clearly, the coefficient at dz in Eq. 40 is the average derivative between mesh points z and $z + dz$ instead of just $\mathbf{E}'(z)$ as in the Euler method. Let us show that this substitution dramatically improves the accuracy of solving Eq. 38. Indeed, Eq. 40 gives

$$\mathbf{E}(z + dz) = \left[I - \frac{1}{2} A(z + dz)dz \right]^{-1} \left[I + \frac{1}{2} A(z)dz \right] \mathbf{E}(z) \quad (41)$$

Assuming that dz is small enough, expansion of the right-hand side of Eq. 40 in powers of dz and substitution of $A(z + dz)$ by $A + A'(z)dz + O(dz^2)$ gives for the GS method:

$$\mathbf{E}(z + dz) = \left\{ I + A(z)dz + \frac{1}{2} [A'(z) + A^2(z)] dz^2 + O(dz^3) \right\} \mathbf{E}(z) \quad (42)$$

On the other hand, expansion of $\mathbf{E}(z + dz)$ in Taylor series gives:

$$\mathbf{E}(z + dz) = \mathbf{E}(z) + \mathbf{E}'(z)dz + \frac{1}{2}\mathbf{E}''(z)dz^2 + O(dz^3) \quad (43)$$

Using Eq. 38, one can find that $\mathbf{E}''(z) = A' \cdot \mathbf{E}' + A \cdot \mathbf{E}' = A'\mathbf{E} + A^2\mathbf{E}$, and Eq. 43 can be rewritten as:

$$\mathbf{E}(z + dz) = \left\{ I + A(z)dz + \frac{1}{2} [A'(z) + A^2(z)] dz^2 + O(dz^3) \right\} \mathbf{E}(z) \quad (44)$$

Comparing Eq. 39 and Eq. 42 with Eq. 44, one finds that the error of computing $\mathbf{E}(z + dz)$ by the GS method that properly accounts for $O(dz^2)$ corrections is $O(dz^3)$. The same error for the Euler method is $O(dz^2)$. Thus, the GS method is one order of magnitude more accurate than the Euler method.

Fig. ?? shows results of numerical integration of Eqs. 5 by the two methods and their comparison with analytical solution (8). Fig. 4 contains numerical solutions obtained by the GS method for $N = 300$ iterations and by the Euler method for $N = 90000$ iterations, when they practically coincide with the analytical curve. Fig. ?? clearly demonstrates the much better accuracy and faster

convergence to the analytical solution when using the GS method as compared to using the Euler method. In a more accurate sense, we define characteristic deviations of the numerically computed curves from the analytical one as $\Delta_N^{GS} \equiv \max |I_N^{GS} - I^{analytical}|$ and $\Delta_N^{Euler} \equiv \max |I_N^{Euler} - I^{analytical}|$ on the interval $4 \leq g \leq 5$, where these deviations are the largest. We found that $\Delta_{N=300}^{GS} \simeq 2 \times 10^{-5} < \Delta_{N=90,000}^{Euler} \simeq 5 \times 10^{-5}$, and $\Delta_{N < 90,000}^{Euler}$ are increasingly larger. The GS method can be successfully used to solve significantly more complicated three-dimensional problems in LCs [14] or elsewhere.

5 Discussion and Conclusions

We have considered light propagation and its transmission through an anisotropic medium: a TNLC. First, an intuitive analytical solution for the light transmission based on dividing the LC slab into a large number of thin sheets was derived. Subsequently, this solution was checked against another approach based on accurate solution for Maxwell's equations applied to light propagation through the LC slab. As shown, the simple formula (Eq. 8) is not generally correct even in the Mauguin limit when the parameter $g = 2d\Delta n/\lambda$ is large. Indeed, as shown in Section III, there is a back-scattered wave originated by the change of the optical axis (LC director) in the direction of light propagation and by the LC birefringence $\Delta n = n_e - n_o \neq 0$. In this case we have two waves polarized along and perpendicular to the director, respectively. These waves have different indexes of refraction, n_e and n_o , which makes it impossible to match them simultaneously with the real part of the refractive index of the polarizer or analyzer. We found that the error of neglecting this contribution is of the order of $(\Delta n/n_e)^2$ and is small when $\Delta n \ll 1$. In this situation, one can neglect it, and the resulting simple formula for the light transmittance is restored. In the final part of the paper, two numerical approaches for solving differential equations were considered. The advantage of the computational Gauss-Seidel method over the Euler approach was shown.

Our approach is trying to clarify particular formulas introduced by books like [10] that are mostly oriented on technical applications and frequently cite formulas without any derivations. At the same time, monographs like¹ are usually dealing only with fundamental aspects of light propagation and do not contain neither formulas for light transmittance through the LC slab nor any details on their technical applications. Thus, our approach to a particular case of the LC physics bridges the gap between the two.

References

- [1] P.G. De Gennes and J. Prost, *The Physics of Liquid Crystals*, 2nd ed. (Oxford University Press, New York, 1993).
- [2] N. Gheorghiu and J.T. Gleeson, “Length and speed selection in dendritic growth of electrohydrodynamic convection in a nematic liquid crystal”, *Phys. Rev. E* **66**, 051710 (2002).
- [3] P.J. Collings, *Nature’s delicate phase of matter*, 2nd ed. (Princeton University Press, Princeton, 2002).
- [4] M. Kleman and O.D. Lavrentovich, *Soft Matter Physics: An Introduction* (Springer, New York, 2002).
- [5] M. Nakata, G. Zanchetta, B.D. Chapman, C.D. Jones, J.O. Cross, R. Pindak, T. Bellini, N.A. Clark, “End-to-end Stacking and Liquid Crystal Condensation of 6-to-20-Base Pair DNA Duplexes”, *Science* **318**, 1276 (2007).
- [6] P. Palffy-Muhoray, “The diverse world of liquid crystals”, *Physics today* **60**(9), 54 (2007).
- [7] V. Hinkov, D. Haug, B. Fauqué, P. Bourges, Y. Sidis, A. Ivanov, C. Bernhard, C.T. Lin, B. Keimer, *Electronic Liquid Crystal State in the High-Temperature Superconductor $YBa_2Cu_3O_{6.45}$* , *Science* **319**, 597 - 600 (2007).
- [8] S.A. Kivelson, E. Fradkin & V.J. Emery, *Electronic liquid-crystal phases of a doped Mott insulator*, *Nature* **393**, 550 - 553 (1998).
- [9] D.J. Griffiths, *Introduction to Electrodynamics*, 3rd ed. (Prentice Hall, New Jersey, 1999).
- [10] I.C. Khoo and S.T. Wu, *Optics and nonlinear optics of liquid crystals* (World Scientific, Singapore, 1993).
- [11] C. Mauguin, *Bull. Soc. Fr. Minér. Crystallogr.* **34**, 3 (1911).
- [12] J.D. Jackson, *Classical Electrodynamics*, 3rd ed., p. 300 (Wiley, New York, 1999).
- [13] C.F. Bohren, D.R. Huffman, *Absorption and scattering of light by small particles* (Wiley, New York, 1998).
- [14] G. Panasyuk, J. Kelly, E.C. Gartland, and D.W. Allender, “Geometrical optics approach in liquid crystal films with three-dimensional director variations”, *Phys. Rev. E* **67**, 041702 (2003).

List of figure captions

FIG. 1. The arrangement of molecules in an uniaxial nematic liquid crystal is described by a unit vector \mathbf{n} known as the *director*.

FIG. 2. Three types of deformation occurring in uniaxial nematics: splay, bend, and twist.

FIG. 3. Twisted nematic liquid crystal layer of thickness d between polarizer P and analyzer A. Inside the layer, \mathbf{n} has a helical structure.

FIG. 4. Comparison of numerical results obtained by the Gauss-Seidel method for $N = 300$ and by the Euler method for $N = 90000$, respectively, to the analytical curve.

FIG. 5. Numerical results show clearly the much better accuracy and faster convergence to the analytical solution when using the Gauss-Seidel method as compared to using the Euler method.

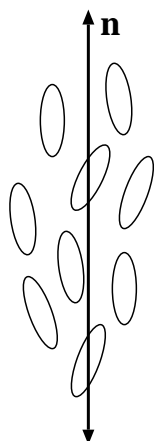
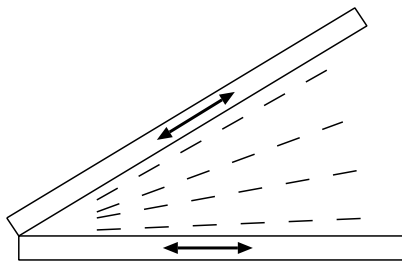
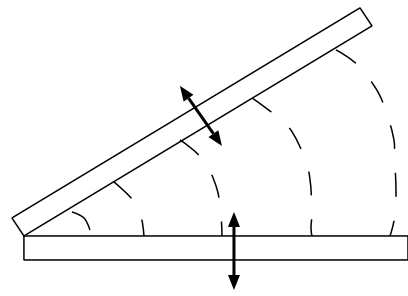


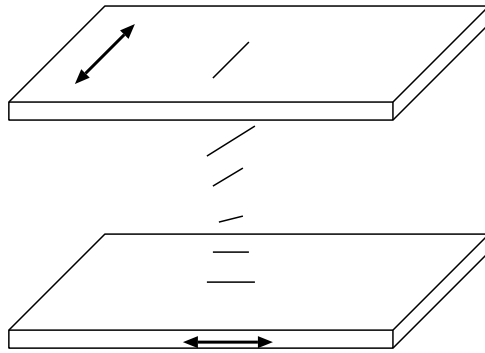
Figure 1:



splay



bend



twist

Figure 2:

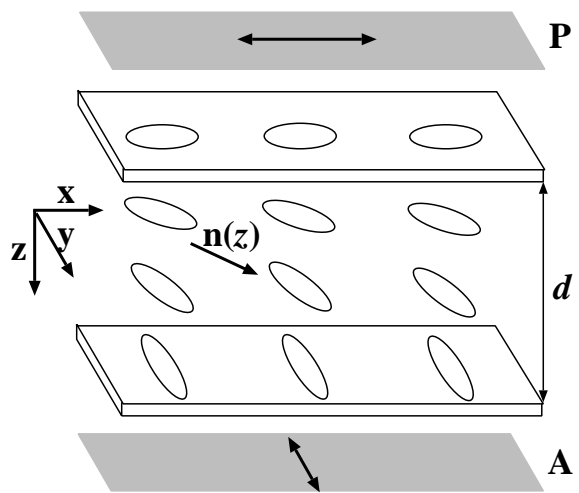


Figure 3:

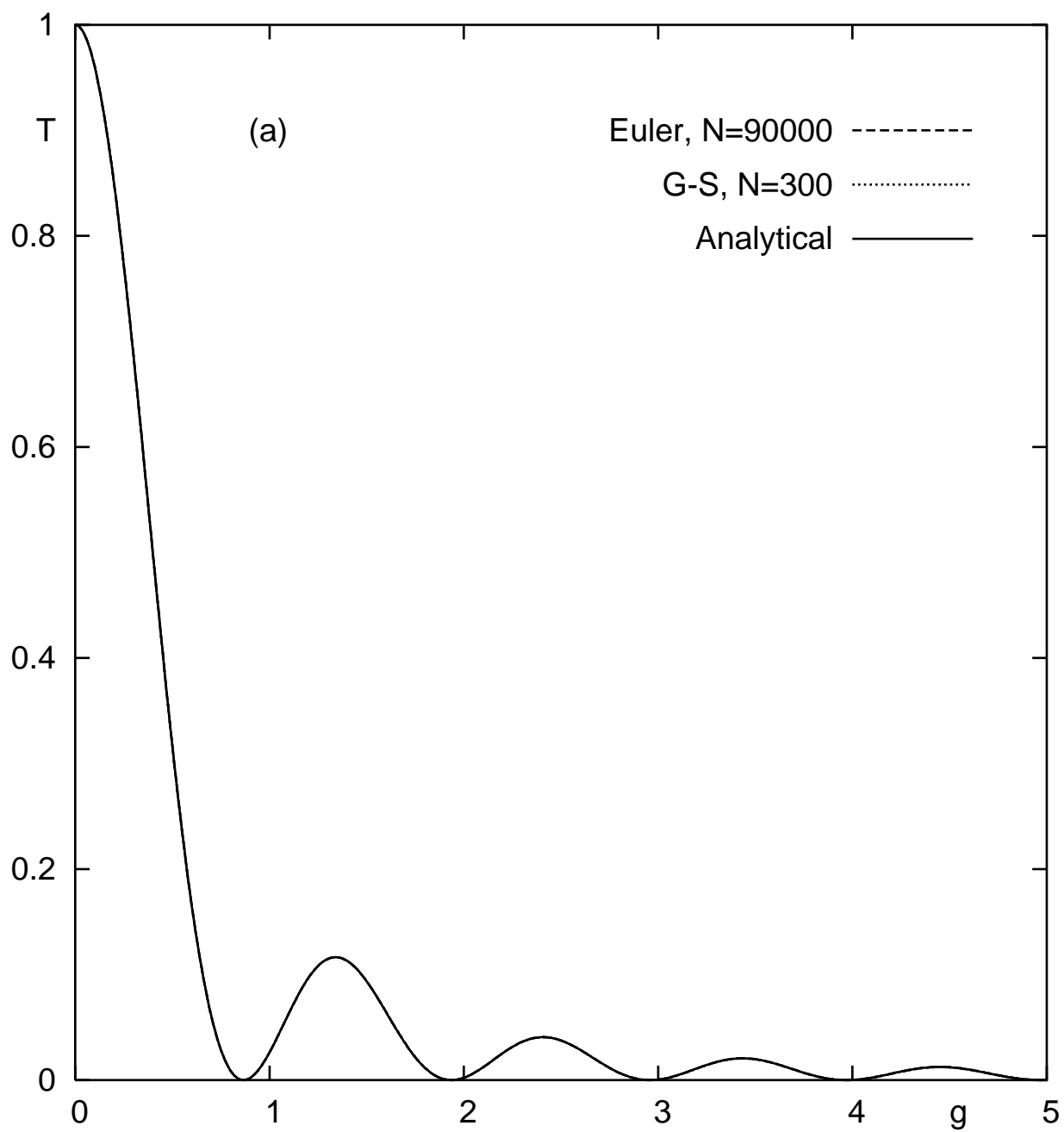


Figure 4:

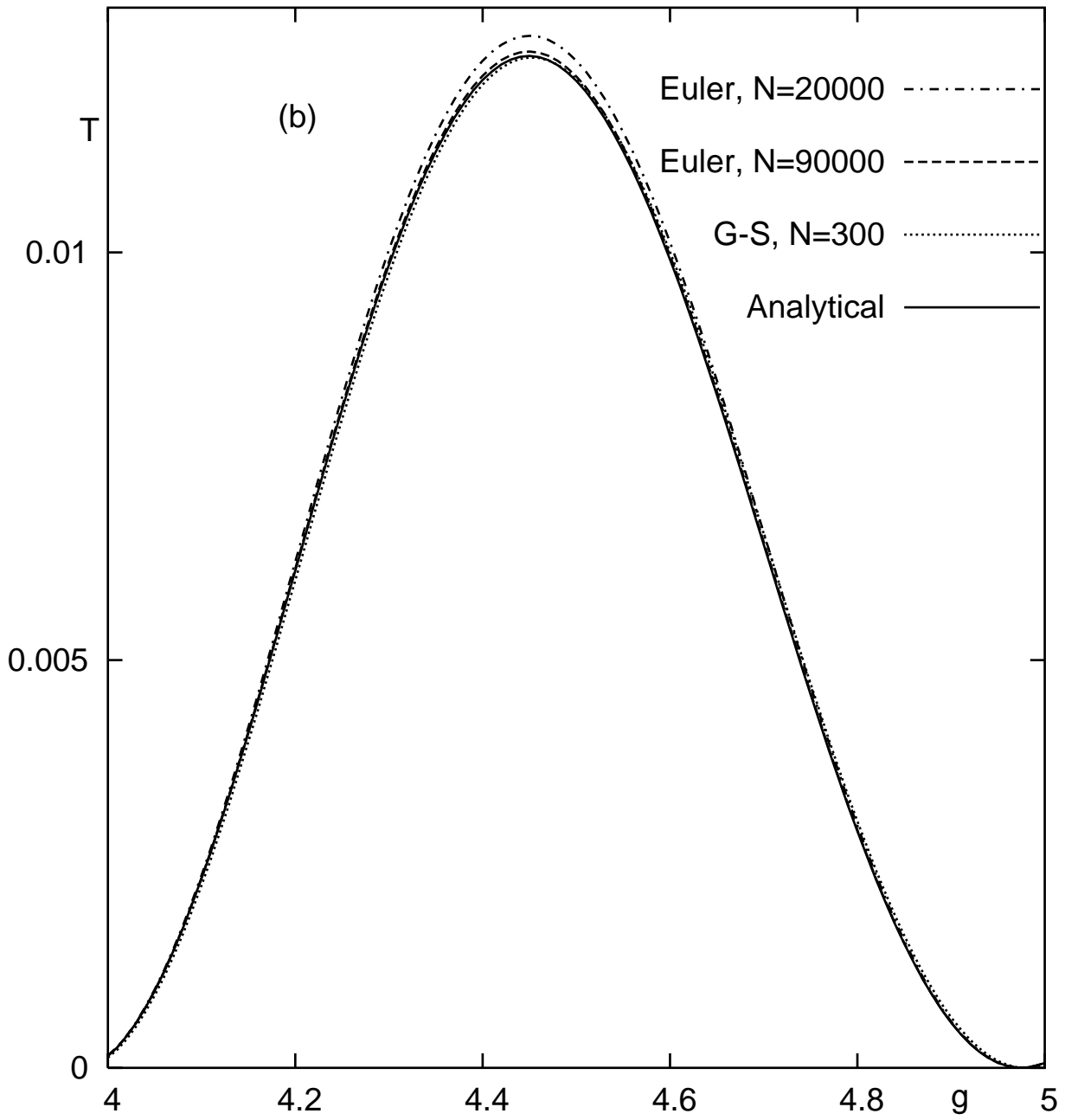


Figure 5: